UNIVERSITÀ DEGLI STUDI DI NAPOLI "FEDERICO II"

Scuola Politecnica e delle Scienze di Base
Area Didattica di Scienze Matematiche, Fisiche e Naturali

DIPARTIMENTO DI BIOLOGIA

Biology of Extreme Environments - Curriculum in Astrobiology

MASTER THESIS
IN
GEOMORPHOLOGY

GEOMORPHICAL ANALYSIS THROUGH AUTOMATIC SEGMENTATION OF SATELLITE AND TOPOGRAPHIC IMAGES FOR DEEP LEARNING BASED CLASSIFICATION

Tutor
Prof. Carlo Donadio

Co-Tutors
Prof. Massimo Brescia
Dott. Stefano Cavuoti

Student
Mariarca D'Aniello

Student ID:
P54000014

Academic Year 2022/2023

SUMMARY

SUMMARY

This thesis delves into the intriguing field of extraterrestrial and terrestrial drainage pattern analysis, shedding light on the hydrogeological and geomorphological histories of celestial bodies such as Earth, Mars, Venus, and Titan. The analysis encompasses both topographic and satellite images, each presenting its unique challenges and requirements.
For topographical images, the study employs image segmentation techniques, specifically focusing on Canny's method with Optical Character Recognition filters, effectively removing symbols and legends from the images. When dealing with satellite images, Canny combined with anisotropic diffusion proves successful in mitigating background noise arising from graininess.

The central objective of this research is the development of mathematical models to automate the segmentation process while preserving drainage network profiles and minimizing information loss. This is crucial for creating a consistent pre-processing phase that can be applied to extensive image datasets, facilitating the generation of a robust training set for classification using self-adaptive machine and deep learning approaches.
In a judicious trade-off between automation and image quality, the study strikes a balance that allows for time-efficient pre-processing of large data volumes. The resultant images are then fed into deep learning models, integrating the extraction and classification phases into an objective and analytical framework. Despite initial challenges posed by limited training data, the similarity of drainage patterns, and noise in the images from automated segmentation, the research yields remarkably impressive results.

The findings ultimately affirm the viability of deep learning as a powerful tool for data exploration in the realm of geomorphology and related fields. This work transcends the confines of terrestrial boundaries, offering valuable insights into the hydrogeological and geomorphological histories of planets and satellites, with the promise of opening new avenues for automated image analysis and data-driven discoveries in the cosmos.

Keywords: Drainage patterns, image segmentation, Canny, Optical Character Recognition, deep learning.

INTRODUCTION

DRAINAGE PATTERN NETWORKS

Extraterrestrial and terrestrial drainage pattern analysis is an interesting topic because it allows us to understand the hydrogeological and geomorphological past of planets and satellites.
In this work Earth, Mars, Venus, and Titan's patterns have been taken in consideration through image segmentation, a field of image analysis specialized in the detection of patterns within images, based on a variety of mathematical methods, whose efficiency depends on the conditions and type of images. In this work, two types of images were addressed, respectively, topographic and satellite.

In both cases, Canny's method (Canny, 1986) has been used with different filters to reduce noise and the one with Optical Character Recognition (Al Sayem A. et al. 2023) provided the best results for topographical images, being able to remove symbols and legends contained in the images.
About satellite images, Canny with anisotropic diffusion showed good results in reducing background noise due to graininess.
The main purpose of this work has been the search for mathematical models capable of automating the segmentation process, making the profiles of the drainage networks stand out from the rest of the image, minimizing the loss of information as well as the variation of the parameters.
This aims to make the preparatory phase of the images (pre-processing) as self-consistent as possible, to be effectively applied to large volumes of images, allowing the generation of a valid training set for the classification of drainage patterns using self-adaptive methods, based on machine and deep learning paradigms (Donadio et al. 2021).

In this work a trade-off has been achieved between automating the pre-processing phase given the large amount of data in a time efficient way and quality of the resulting images. These latter images have been fed to deep learning models, in which the extraction and classification phase is integrated within a more objective, analytical, and automatic framework.
Despite the initial difficulties, due to the small number of training images available, the similarity between the different shapes of the drainage samples, as well as the noise in most images due to automatic segmentation, we obtained very promising results, confirming that automatic segmentation and deep learning-based classification are a robust framework for data exploration in geomorphology and related fields.

AN EXTRACTION AND CLASSIFICATION PROBLEM

To study and reconstruct the morphological history of the planet of interest, it is noteworthy to analyze drainage pattern images to extract their profiles and therefore be able to determine the direction of flow, the depth, the approximated speed of the fluid flowing there, and other characteristics related to these structures (Burr et al. 2009; Burr et al. 2013).
The efficiency of computers has been used to speed up this work and to obtain better results in the lattice profile extraction.
The ideal technique for this purpose is segmentation, which allows the input image to be divided into various areas of interest, depending on the chosen method. In the following sections, the Canny algorithm will be explained in more detail, along with the main filters used in this project. As expected, different filters will result in different output images, sometimes for the better, sometimes worsening the result.

The scientific problem of an unbiased classification of drainage networks is characterized by the two mentioned aspects, approached through Deep Learning (DL) in our research. Different from other methods, by adding data, the DL model reinforces the learning power based on its acquired experience, which is used to generalize the ability to classify new samples, thus improving the accuracy and reliability of the classification of new drainage patterns. Such method, directly applied to images, has the real potentiality to define a new, more objective classification of these complex natural elements, characterized by an irregular and asymmetrical geometry, thus contributing to a better characterization and analysis of terrestrial and extraterrestrial examples. In such a scenario, the primary objective of the present work is to classify the drainage networks in an unambiguous, reliable, and as automated as possible way. Unambiguous means guaranteeing the utmost accuracy in assigning the right class, in accordance, but also on a complementary base, with the broadest and most objective consensus provided by the community of experts in the field. To reach this consensus, this work intends to promote the "River Zoo" survey initiative, aimed primarily at involving the entire scientific community interested in the field and inspired by the well-known category of "citizen science projects".

The idea behind such an initiative is mostly to solve the problem of the current lack of drainage network samples useful for facing the exercise of multi-class classification in a statistically consistent and balanced way. Therefore, multiple participation in the expert survey would be able to guarantee a more reliable assignment of the class to each sample, improving the quality and ensuring an incremental strengthening of the training set for DL models.

The DL approach is also able to guarantee the repeatability, coherence, and consistency of classification, by maximizing the incremental acquisition of experience (incremental learning), thus ensuring the application of same and consolidated criteria to other drainage network samples over time. Furthermore, another significant

aspect of the presented method is to exploit the aseptic and complete information deriving directly from the analysis of the images, avoiding the use of potentially biased, incomplete, and ambiguous derived information, i.e., traditionally extrapolated from processed physical and environmental parameters.

Finally, the method is intrinsically automated, thus able to minimize the human intervention in the classification process, relegating it to an a posteriori analysis and the scientific exploitation of the results obtained. Certainly, the long-term goal of the project, for which this work is a fundamental premise, is the multi-class classification using at least the taxonomy highlighted in Fig. 1. However, now, the intrinsic complexity of distinguishing between sub-classes due to the ambiguity in the morphology of the patterns and the subjectivity of the attribution of the class, does not allow to have a quantity and quality of examples for each sub-class sufficient to allow the multi-class experiment to be carried out.

As is well known, the supervised paradigm of DL requires an adequate number of known examples for each sub-class and requires the fairest possible balance between the quantities of examples for each sub-class. Without this knowledge base, any data-driven method of classification would suffer from underfitting for the under-sampled classes and overfitting for the over-sampled ones. For these reasons, the present work was focused on testing and validating the proposed data-driven method on the reduced two-class problem to distinguish between two families of drainage network sub-classes named, respectively, dendritic and non-dendritic.

Moreover, without the experience acquired with this first case, it would be extremely difficult to analyze the results of the more complex multi-class experiment and identify the weaknesses of the method, disentangling the different contributions to the multi-classification error between data-induced errors from those induced by the DL models (Donadio et al.,2021).

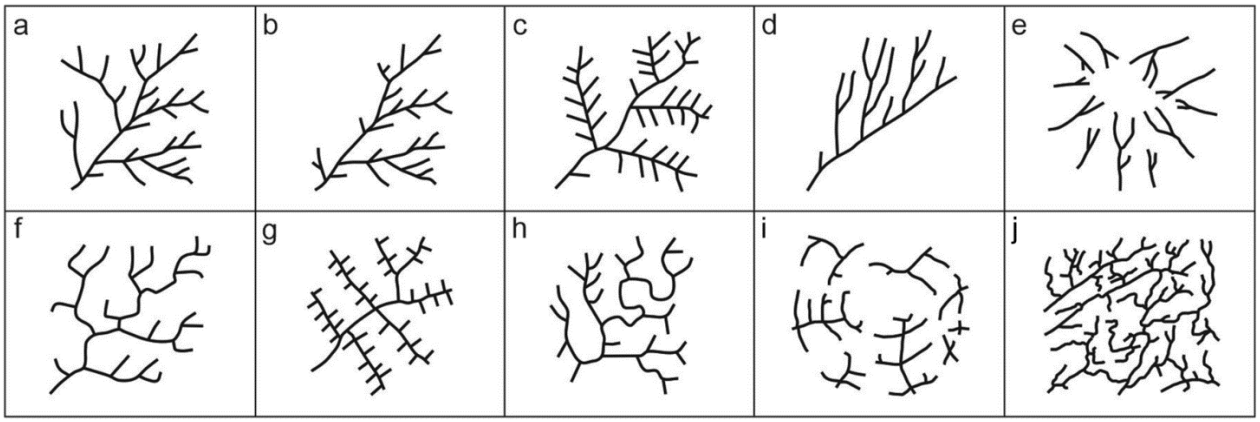

Fig.1 Main patterns of drainage networks: (**a**) dendritic; (**b**) sub-dendritic; (**c**) pinnate; (**d**) parallel; (**e**) radial; (**f**) rectangular; (**g**) trellis; (**h**) angular; (**i**) annular; (**j**) contorted. Hereinafter (**a**)–(**c**) patterns are related to dendritic forms (D), (**d**)–(**j**) to non-dendritic ones (ND).

AIMS

The aim of this work encompasses several key objectives, which collectively contribute to the advancement of river hydrogeological profile extraction and geomorphological feature classification. These objectives are the enhancing hydrogeological profile extraction: the primary objective is to improve existing methods for extracting hydrogeological profiles of rivers using the Edge Detection technique.
This enhancement involves refining the precision and clarity of the extracted profiles, ensuring that the contours are distinct and well-defined. Achieving this goal will facilitate more accurate geomorphological analysis. Then, the exploration of Deep Learning approaches.

In addition to traditional Edge Detection techniques, this study explores the application of deep learning methods to extract hydrogeological profiles. DL models have demonstrated remarkable capabilities in image feature extraction and pattern recognition. The aim is to develop novel methods that leverage deep learning to automate the extraction process, potentially leading to even more pronounced and detailed profile lines.
Another overarching objective is to automate the extraction of hydrogeological profiles entirely.
By achieving automation, the process becomes more efficient and less reliant on manual intervention. This automation contributes to expediting the analysis of river geomorphology. Geospatial Image Classification played an important role beyond profile extraction. This work delves into the broader realm of geospatial image classification.

The study extends to the automatic segmentation and classification of various geomorphological features within satellite and topographic images. This includes distinguishing dendritic river patterns from mixed patterns and other relevant classifications. The comparative analysis allowed us to assess the efficacy of automated segmentation and classification; this research conducts a comparative analysis. It involves comparing the results obtained through automated techniques with those from manual segmentation performed by a colleague. The aim is to discern the trade-offs and advantages offered by automation in terms of classification accuracy, efficiency, and precision.

In the end, preliminary stages in geomorphological analysis is important to recognize that the extraction process involves several preliminary stages to obtain a well-defined contour. These stages encompass data preprocessing, noise reduction, and image enhancement. The aim is to ensure that the data is optimally prepared for subsequent analysis, which is essential for accurate geomorphological assessments. By addressing these aims and objectives, this research aims to contribute to the field of geomorphological analysis by leveraging advanced techniques to streamline the extraction and classification of hydrogeological profiles and other relevant features. The outcomes are expected to provide valuable insights into the potential benefits of deep learning in geospatial analysis and feature recognition.

MATERIALS AND METHODS

A COMPREHENSIVE REVIEW OF THE CANNY EDGE DETECTION ALGORITHM AND USAGE OF DIFFERENT FILTERS

The Canny edge detector is an edge detection operator that uses a multi-stage algorithm to detect a wide range of edges in images. It was developed by John F. Canny in 1986. Canny also produced a computational theory of edge detection explaining why the technique works. It is a technique to extract useful structural information from different vision objects and dramatically reduce the amount of data to be processed.

The process of Canny edge detection algorithm can be broken down to five different steps:

I) Apply a filter to smooth the image to remove the noise. In this case, I used **anisotropic diffusion**, **Bregman** and **non-local means** filters.

II) Find the intensity gradients of the image and its magnitude. The gradients provide information about the intensity variations and changes in the image.

III) Apply gradient magnitude thresholding or lower bound cut-off suppression to get rid of spurious response to edge detection.

IV) Apply double threshold to determine potential edges. To make an automated calculation, I used **median** and **standard deviation**.

V) Track edge by hysteresis: Finalize the detection of edges by suppressing all the other edges that are weak and not connected to strong edges (fig.2).

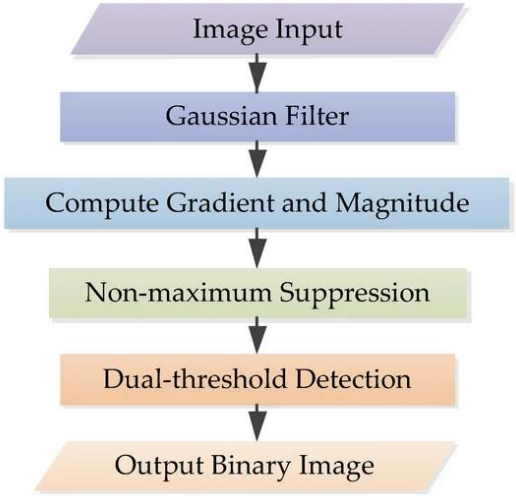

Fig.2 Flowchart of the traditional Canny algorithm

The **anisotropic diffusion filter** (Perona P., Malik J. 1987) is based on a diffusion process, a kind of non-linear smoothing. The diffusion speed can be adjusted in a way that it does not affect the edges as much as other filters, hence preserving them. It requires input parameters; each one needs to be tuned correctly to produce a great image:

- Niter: determines how many iterations of the algorithm will be executed.
- Kappa: is the conduction coefficient, varying between 20 and 100. If low, diffusion across step edges is blocked, because small intensity gradients can block conduction.
- Gamma: controls the speed of diffusion. Max value 0.25 for stability.
- Option: if 1, the first Perona-Malik diffusion equation is used, which favors high contrast edges over low contrast ones; if 2, the second equation is used, which favors wide regions over smaller ones.
- Sigma: if <0 then Gaussian Noise removal is applied as well.

There may be several techniques to make this method automated. The one that I used is based on the search for every possible combination of the 5 parameters earlier described for each of the 161 images, in fixed intervals. Each parameter varies in a list of three elements, in which the first and the third value deviate equally from the second, respectively by subtracting and adding a numerical constant.

From each of 23 satellite images, I got 3^4 = 91 different outputs, for a total of 2093. After that, one can perform a statistical analysis on the parameters with different indexes such as average, median, mode, standard deviation to find what kind of combination best fits with most of the 161 images. After several experiments, the method is efficient in revealing the rivers but not in reducing background noise.

The **Bregman denoising filter** (Deng G., Broadbridge P. 2019) is a mathematical technique based on the Bregman distance, which is a measure of dissimilarity between two probability distributions: noisy and denoised images. The method aims to minimize the Bregman distance between a noisy image and its denoised version by iteratively updating the denoised image. It considers the non-linearity and geometry of the image data, enabling more effective and accurate processing and analysis of images.

The **non-local means filter** (Buades A. 2005) performs non-local means denoising on grayscale or RGB images. It is based on the principle that similar patches within an image exhibit similar intensity pattern and leverages this self-similarity property to estimate the original, noise-free pixel values. It is a non-Destructive Denoising: unlike some denoising methods that may blur or distort edges and boundaries, NL means denoising generally maintains sharp edges and boundaries in the denoised image. It achieves a good balance between noise reduction and preservation of important image features. The filter requires parameter tuning: the denoising strength can be adjusted by controlling parameters such as the patch size, similarity measure, and filtering strength that have been made constant.

CANNY WITH OPTICAL CHARACTER RECOGNITION

In image segmentation, **Optical Character Recognition** (OCR) is used to enable computers to "read" and understand text that appears in images, making it possible to extract information from documents, images with embedded text, or any visual content that contains textual information (fig.3).

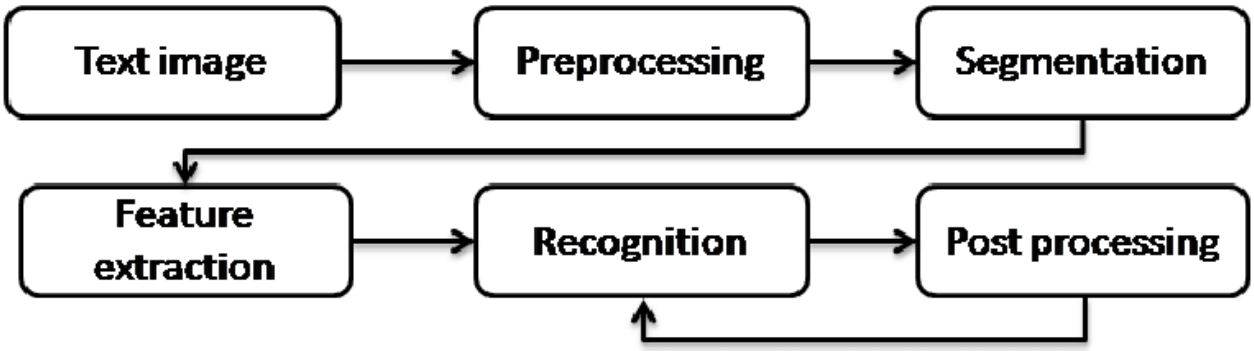

Fig. 3 Phases of character recognition process.

In the topographical images, it has been useful in recognizing letters, symbols, and legends. For my purpose, I have implemented a method in which in the first part text recognition is done, while in the second part the edge detection is performed. Here is the algorithm:

I) Set a confidence level: too low or too high won't let the OCR detect all the text or worse, detect some elements as characters while clearly, they are not text.

II) Select a Page Segmentation Mode (6 & 11), then perform OCR. PSM 6 focuses on finding blocks of columned text. This pattern is often used to write legends and general symbology in topographical images. PSM11 is used to recognize "Sparse text with no particular order".

III) Letter and phrases are covered by white rectangles to remove them.

IV) Edge detection with Canny: threshold with median which is one of the most stable indicators of a probability function. It is the closest value to the distribution (center) considering a first-order distance.

V) Detect contours using cv2.

VI) Perform a contour shape evaluation and writing on mask that basically accumulates everything to then remove (if needed).

VII) Subtract mask from edged image and invert colors.

DEEP LEARNING APPROACH

In the realm of Artificial Intelligence (AI), Machine Learning (ML) has played a crucial role in solving complex problems that can be challenging for humans but relatively simple for computers. This has become particularly important in scientific research due to the vast and diverse datasets now available. In scientific applications, the quality of ML models depends on how well they represent data. DL, a subset of ML, has become popular because it not only extracts meaningful information from data but also makes accurate classifications. This is especially useful when experts can recognize patterns in images, but manually analyzing each image is impractical or when capturing and categorizing all relevant information numerically is challenging.

For the classification task, supervised DL methods have been employed, utilizing two well-established convolutional neural network architectures, VGGNet (fig.4) and AlexNet (fig.5). These models were utilized to assign class labels to the collected Earth examples, distinguishing between two classes: dendritic (D), including subtypes such as sub-dendritic, pinnate, and high-relief pinnate, versus not-dendritic (ND), encompassing other subtypes such as trellis, parallel, rectangular, angular, annular, radial, centripetal, herringbone, and barbed.

To ensure an ample supply of training samples, we applied data augmentation techniques to enhance the model's training capabilities.

This augmentation process involved resizing all images to a uniform 540 × 540 pixels and generating five additional samples for each original image through three 90-degree rotations, 180-degree rotations, 270-degree rotations, and two flipping operations along the horizontal and vertical axes.

This approach not only increased the dataset size but also made the trained model invariant to different orientations of drainage networks within the images. Additionally, we vectorized the images to represent the network morphology in a simple yet informative and quantitative form, converting them to grayscale to facilitate the extraction of the network pattern.

Subsequently, the images underwent a cleaning process to eliminate residual noise and to restore parts of the reticle that may have been partially lost during the conversion. Then, two separate experiments were conducted to assess the performance of the models described above.

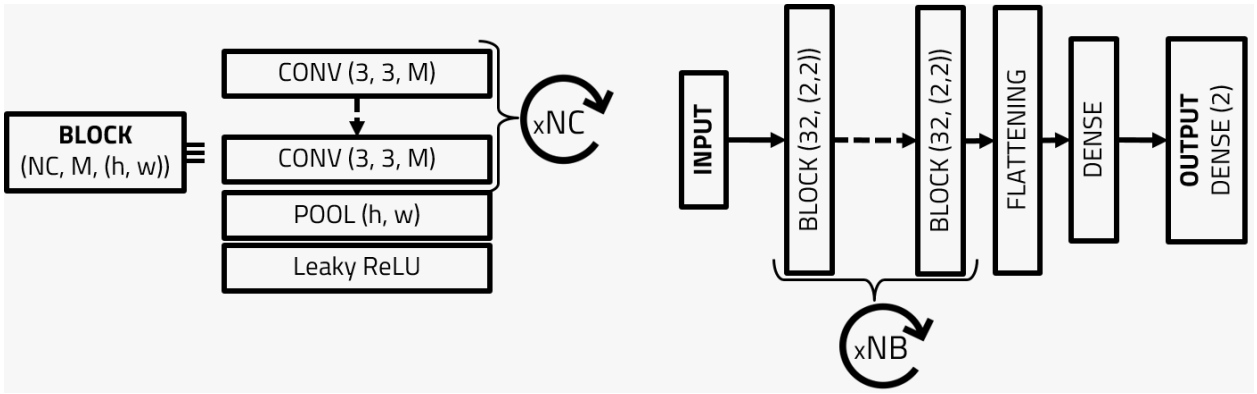

Fig. 4 CNN VGGNet (Simonyan K., Zisserman A. 2014).

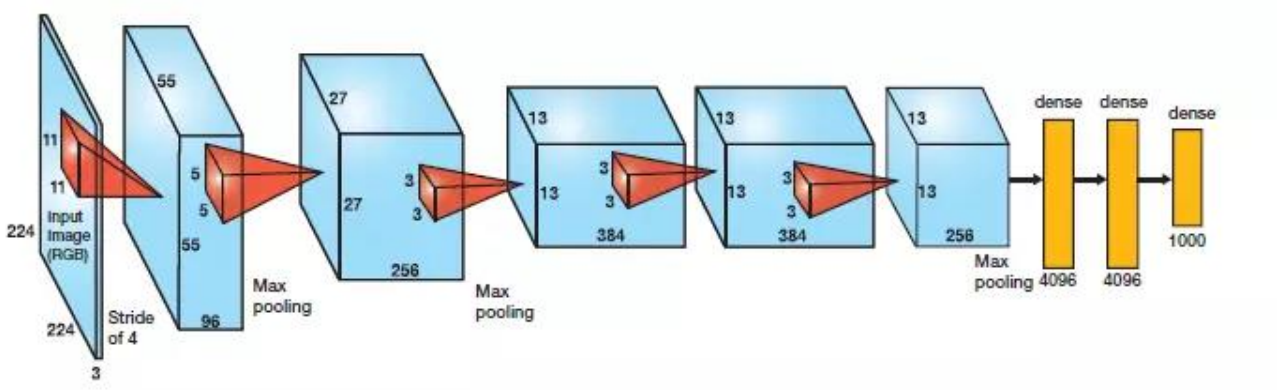

Fig. 5 CNN Alexnet (Krizhevsky A., Sutskever I. 2012).

In this study, various DL models and optimizers were tested, including VGGNet + ADAM, VGGNet + Random Forest, AlexNet + ADADELTA and others. These models automatically extract features from images and then classify them based on those features. The classification results are presented as probability matrices, with each image assigned probabilities for belonging to different classes.

The models are trained using the cross-entropy error function (Goodfellow et al. 2016):

$$C(y,\bar{y}) = \sum_{i=1}^{N_{classes}} (y_i * \ln(\bar{y}_i) + (1 - y_i) * \ln(1 - \bar{y}_i)) \quad (1)$$

Three classification algorithms or optimizers — Adagrad, Adadelta, and ADAM—were evaluated. The assessment included metrics such as precision, recall, and F1-score, which help measure how accurately the models classify images.

Recall and precision are the two most interesting estimators. Recall measures the ability to detect True Positive samples, while precision estimates the ability to select a set of candidates of a single class, thus minimizing the level of induced contamination from classification errors i.e., the presence of false positives and false negatives.

Assuming TP the number of samples correctly classified as class P, TN the number of samples correctly classified as class N, FP the set of samples incorrectly classified as class FP while considering FN the samples incorrectly classified as class N, and given P and N the sizes of respectively class P and class N, the metrics can be calculated as follows:

$$Precision = \frac{TP}{TP+FP} \quad (2)$$

$$Recall = \frac{TP}{TP+FN} \quad (3)$$

$$F1 = \frac{2TP}{2TP+FP+FN} \quad (4)$$

Furthermore, it is often useful building a Confusion Matrix to graphically evaluate those metrics. Although this technique is quite diffused, here different graphic means of visualization have been used, as will be discussed later. For reference, fig.6 illustrates an example of Confusion Matrix.

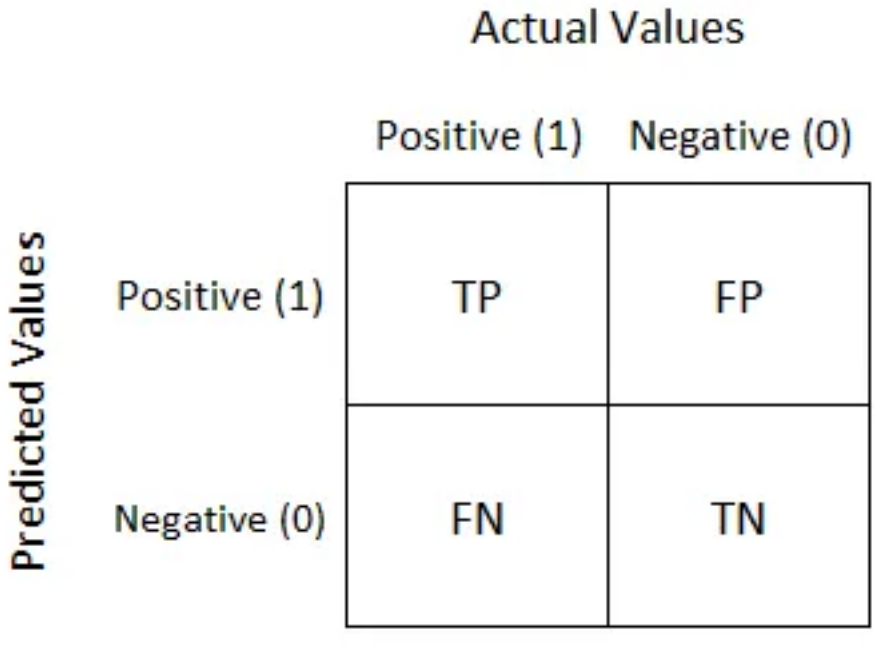

Fig.6 Example of a confusion matrix for a two-class problem.

The quality of classification is based on the best compromise between these two estimators. Statistical evaluation was completed by introducing ROC diagrams (Receiver Operating Characteristic; Hanley & McNeil 1982), whose curves allow us to evaluate the level of classification as the discrimination threshold attributed to distinguish membership of the two classes. The value total statistic is measured by the area under the ROC curve (AUC), where an area equal to 1 indicates a perfect classification, while a value of 0.5 indicates a random classification (fig.7).

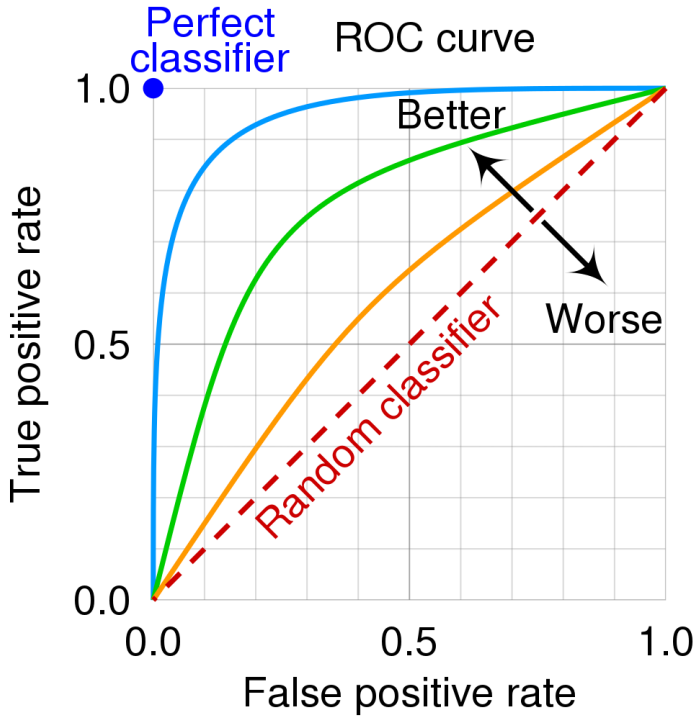

Fig.7 Receiver Operating Characteristics (ROC curve)

In this project, a total of 165 images have been used to assess the models' performance with noisy and imperfect data. For comparison, the work prior to this one achieved near-perfect results using DL models trained on manually segmented images. Of course, automatic segmentation produces worse results than manual, nevertheless we were able to extract rivers' profile with enough accuracy to successfully train the models, subsequently achieving good results while testing. The focus of this work was to determine whether the two models could perform reasonably well on dataset of automatically segmented images. The outcome, as will be discussed later, was good, obtaining a precision of around 80% ~ 90% percent while training, and producing ROC curves situated in the top-left portion of the chart.

As for the datasets, the models need three sets of images. The first one, referred to as training set, is typically the largest; here, 75% of the 165 images have been used to train the model, giving a baseline of 124 training

images. The smallest dataset, known as validation set, is not mandatory to use, but it is useful to evaluate real-time performance of the classification algorithm while it is still training; in this thesis the validation set is composed of 7 images, roughly 4% of the total. Finally, there is the testing set, taking up the rest of the images, 34 in this case. The testing set is the real evaluation method of a model's analysis, given that a DL algorithm (in this case a binary classifier) has the responsibility of labeling each image in this set with the corresponding class of rivers. The better the model's architecture and the optimizer, as well as the image quality, the closer the classification will be to the ground truth.

Once the datasets are created, data augmentation algorithms are responsible for increasing the number of training samples. Given the size of the training set used in this project, the augmentation phase outputs more than 700 images. Since the entire dataset has to be loaded into RAM (Random Access Memory) memory to be used, and that AlexNET (the most complex architecture used in this work) can have Dense Convolutional Layers of up to 4096 cells, it is obvious that such a dataset can heavily impact the CPU (Central Processing Unit) of a computer. For this reason, it is extremely recommended to run the algorithm on Nvidia GPUs (Graphic Processing Units), to take advantage of the parallel processing capabilities of CUDA (Compute Unified Device Architecture) cores and Tensors.

As a reference, I have used a Nvidia RTX 3060 GPU with 12GB of dedicated VRAM (Virtual RAM), and the datasets barely fit in the memory, but the algorithm ran extremely fast even at small batches, taking a consistent 5 seconds for each training epoch.

In the next section, the results will be presented. As mentioned before, different optimizers have been used, each time with different parameters, especially focusing on batch size and epochs count. The smaller the batch size, the more accurate the learning will be, at the expense of loading the entire training set into memory at run time; higher batch sizes provide faster learning at the expense of overall accuracy. As for epochs, they correspond to the iterations of the learning algorithm. It must be noted that more epochs do not necessarily mean better overall results.

The model could be learning so much on the same data that it could get confused and "too confident" that most of the images belong to just one class, producing incorrect classification. This phenomenon is called **overfitting**.

The opposite, **underfitting**, occurs when the model learns so little that it almost "guesses" its predictions. As the reader will soon see, I have found optimal values of these two parameters, thanks to a process of optimization called Grid Search.

RESULTS

In this section, I have provided a concise overview of the results obtained from the automated segmentation of river drainage patterns and the subsequent classification achieved through DL models. The key highlights of this section include the identification of the most effective automated segmentation method and the impressive accuracy achieved when using DL models to analyze these segmented images.

IMAGE PRE-PROCESSING AND FILTRATION

In this part, we present a preliminary stage of segmentation, featuring a selection of 165 satellite and topographical images that have undergone preprocessing. These images were resized to a uniform size of 540x540 pixels and converted from RGB to grayscale to facilitate the subsequent segmentation processes. Prior to segmentation, these preprocessed images were filtered using four distinct methods. These filtered images serve as the foundation for our comprehensive segmentation analysis.

Before presenting the results of this preliminary phase, it must be noted that all the resulting images have been resized to 540x540 pixel to have the same size as the input dimension of the Neural Networks. For most images, a stretching has been performed, while some images have been padded to avoid loss of important details.

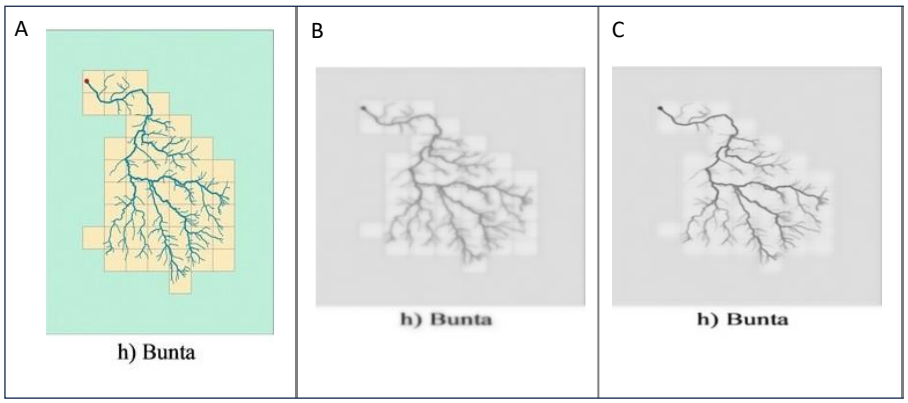

Fig. 8 A) Original topographic image of Bunta river B) Bunta river filtered with Bregman denoising filter C) Bunta river filtered with non-local means

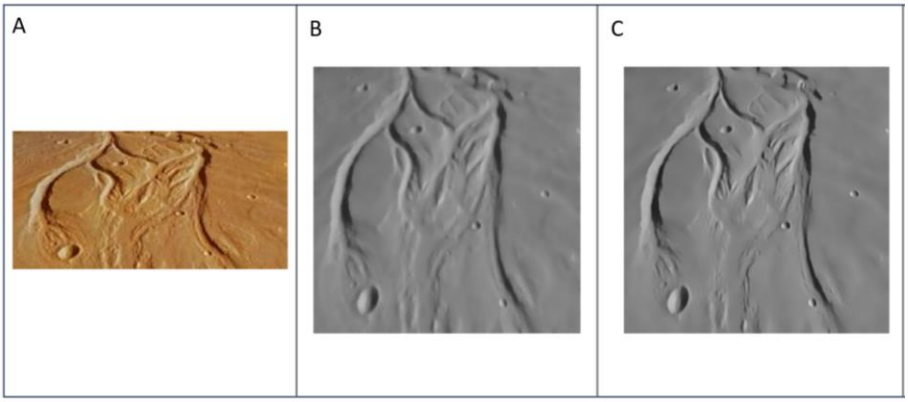

Fig. 9 A) Original satellite image of Gale River B) Gale river filtered with Bregman denoising filter C) Gale river filtered with non-local means

In our extensive analysis of 165 images, it became evident that the Bregman and NL-means filters exhibited a wide range of performance, yielding both suboptimal and satisfactory results. Specifically, these filters produced favorable outcomes for some images while falling short for others (Fig.8-9).

After several analysis, we found that none of the filters were suitable for widespread adoption in our segmentation approach, as their inconsistent performance across image types would likely introduce confusion to the subsequent DL models.

Nevertheless, it's worth mentioning that in the upcoming sections, we will introduce a novel method called OCR that demonstrated high efficiency across a broader spectrum of images. This promising approach offered the potential to address the segmentation challenges posed by diverse image types, further enhancing the reliability of our DL models.

IMAGE SEGMENTATION

In this section, I present a set of segmented images obtained through the Canny edge detection method, following the application of various filters as a preliminary step. These segmented images serve as illustrative examples, building upon the previously discussed filtered images, showcasing the effectiveness of the segmentation process in highlighting distinct features within the images.

Fig.10 A) Original satellite image of Gale river B) Bunta river image analyzed with Bregman filter and segmented with Canny method C) Bunta river analyzed with non-local means filter and segmented with Canny D) Bunta river analyzed anisotropic filter and segmented with Canny

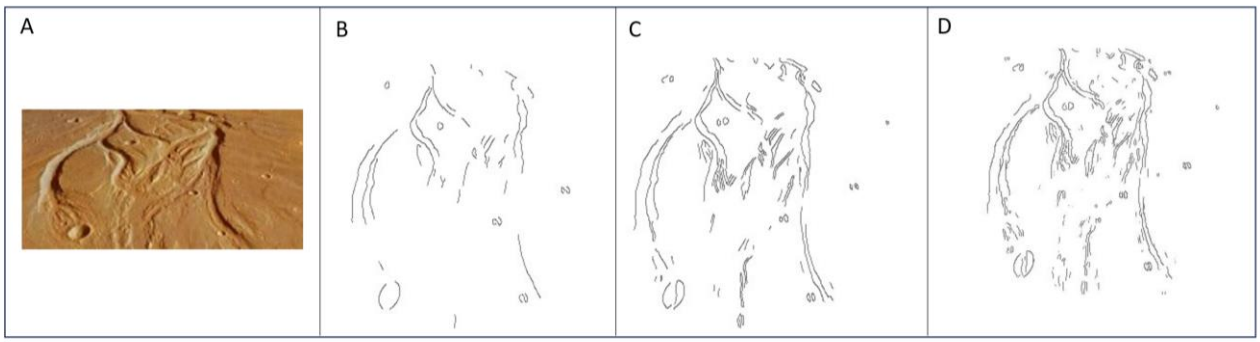

Fig.11 A) Original satellite image of Gale river B) Gale river image analyzed with Bregman denoising filter and segmented with Canny method C) Gale river analyzed with non-local means filter and segmented with Canny D) Gale river analyzed anisotropic filter and segmented with Canny

As we examine these images, it becomes evident that the application of the Bregman denoising filter did not yield the expected results. Despite its potential to minimize the dissimilarity between noisy and denoised images, as measured by the Bregman distance, this method proved less effective in our specific context. The challenges encountered with the Bregman filter might be attributed to the unique characteristics of our images or the interactions with subsequent segmentation processes. It is essential to acknowledge that the performance of this filter can vary depending on the specific nature of the input data and the processing steps involved. In our case, the results fell short of our expectations, prompting further exploration of alternative image enhancement and segmentation techniques.

Meanwhile, we observe that the application of the non-local means filter, with constant parameters, has produced noteworthy results. This filter operates on the principle that similar patches within an image share common intensity patterns and leverages this self-similarity property to estimate the original, noise-free pixel values. One of the distinct advantages of this method is its non-destructive denoising nature. Unlike some denoising techniques that may blur or distort edges and boundaries, the non-local means filter generally preserves sharp edges and boundaries in the denoised image.

It is important to note that, with constant parameters, the non-local means filter has proven effective in enhancing a substantial portion of our images. However, it did not exhibit uniform performance across all 165 images. This variation in results may be attributed to differences in image characteristics and noise levels.

Basically, as we can see in these images, the non-local means filter with constant parameters has successfully achieved a good balance between noise reduction and the preservation of important image features. However, its performance may still vary, underscoring the potential for further optimization to maximize its effectiveness on different types of images.

In the end, we see that it's apparent that the anisotropic filtering and subsequent segmentation using the Canny edge detection method have effectively highlighted the river patterns within the images. The anisotropic filter has proven efficient in revealing these intricate river structures.

In particular, the anisotropic filters demonstrated their efficacy in enhancing satellite images, delivering notably improved results. However, they proved less efficient when applied to topographical images, primarily due to their inability to effectively eliminate noise, such as characters and letters. Given the predominance of topographical images in our dataset compared to satellite images, we decided against adopting anisotropic filters for the overall segmentation process.

However, it's important to note that the same efficiency in revealing river patterns has limitations when it comes to removing background noise effectively. The presence of residual noise and artifacts in the segmented images is noticeable, which poses challenges for further processing, particularly when feeding these images into DL models (Fig.10-11).

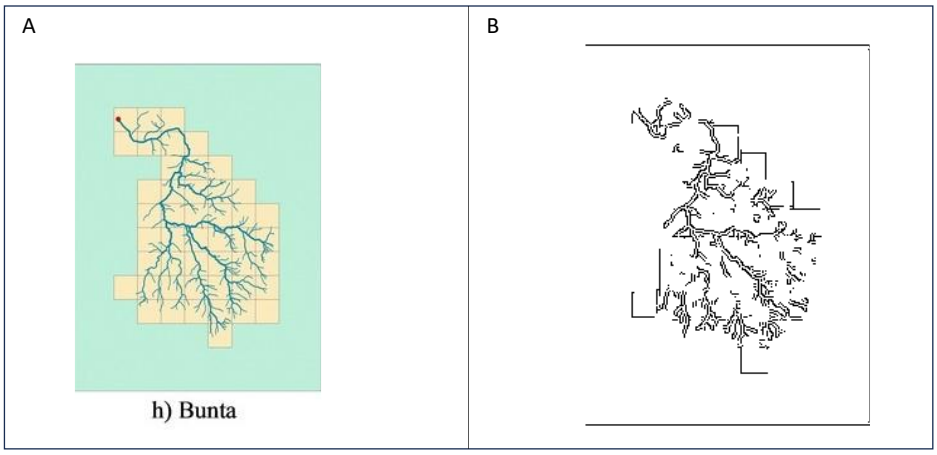

Fig.12 A) Original topographic image of Bunta river B) Bunta river analyzed with OCR method and segmented with Canny

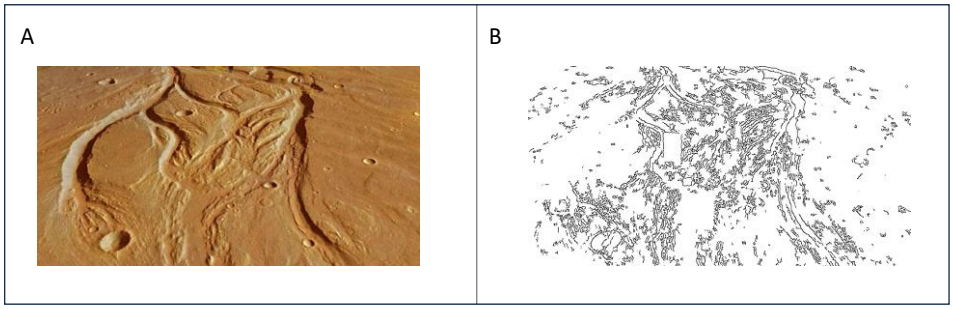

Fig. 13 A) Original satellite image of Gale River B) Gale river analyzed with OCR method and segmented with Canny

As part of our ongoing investigation, we delved into the efficacy of the OCR (Optical Character Recognition) method in image enhancement and segmentation. Our aim was to understand how this method performs in the context of our diverse image dataset, comprising both topographical and satellite images.

However, our findings took a different turn when we applied the OCR method to satellite images. These images, in contrast to topographical ones, lacked the presence of characters, letters, legends, or similar textual elements. As a result, the OCR method proved unsuitable for this specific image type (Fig.12-13).

Considering these notable distinctions in performance, we made a strategic decision. We chose to utilize the segmented images generated through the OCR method, in conjunction with the Canny edge detection method, as inputs for our DL models. This decision allowed us to leverage the strengths of OCR in enhancing topographical images while accommodating the unique characteristics of satellite imagery. The combined approach served as a vital step in streamlining the DL model training process.

DEEP LEARNING

Before discussing the results, let's first take a look at the input images. The following table shows the drainage pattern for each river in light green. This is also called **ground truth**, and derives from an evaluation of an expert. Dendritic rivers are labeled with a D with a light blue background, while non dendritic (mixed) patterns are labeled with a ND and orange background.

Name	Label	Name	Label	Name	Label	Name	Label
Achankovil	D	Huasco	D	NagtonVallei	ND	Tanaro	D
Aconcagua	ND	HuygensCrater	D	Neyyar	ND	Tarali	ND
Adda	D	Idice	D	Niger	D	TerraCimeria	D
Adige	D	Indus	D	Nile	D	Tevere	ND
AeolisPlanum	ND	IndusVallei	ND	NirgalVallis	ND	Thames	D
AlAbiadh	ND	Isonzo	D	Ob	D	Ticino	D
Amazon	ND	Itata	D	Oder	D	Tigri	D
Amur	D	Jharkhand	ND	Ohio	D	Titan	ND
AnjaniandJhiri	ND	Jordan	D	Olenek	D	Titan2	ND
ArabiaQuadrangle	D	Kadalundi	D	Ombrone	D	Toaya	D
Arno	D	Kadvi	ND	Orr	ND	Tobol	D
Bahomoleo	D	Kallada	D	OsugaVallis	D	Turkey	ND
Bangga	ND	Karamana	D	Ottawa	ND	TyrasValley	ND
Basento	D	Karuvannur	ND	Pamba	D	Umbro	ND
Bharathapuzha	ND	Kaveri	D	Paraguay	ND	Uruguay	D
Biobio	D	Kentucky	ND	ParaibadoSul	D	Vamanapuram	ND
Blanchard	ND	Kolyma	D	Parana	D	Varuna	ND
Bouquet	ND	Krishna	D	ParanaValley	ND	VenereC	ND

Bradano	D	Kuttiyadi	ND	Periyar	D	VenereD	ND
Bunta	ND	Lena	D	Petrace	ND	VenereE	ND
Candelaro	ND	Liri	D	Piave	D	VenereF	ND
CaptinaCreek	ND	LockrasVallei	D	Pinamula	ND	VenereG	ND
Chalakudy	D	Loire	ND	Pinios	D	VenereH	ND
Chaliyar	ND	Luni	D	Po	ND	Vergas	ND
Chari	D	MaadimVallis	ND	Powder	ND	Vishwamitri	ND
ChrysePlanitia	D	MaadimVallis2	D	Rapel	ND	Vistula	D
Congo	ND	Mackenze	D	Rhine	D	Vjosa	D
Cususvalles	D	Mahe	D	Rhone	ND	Volga	D
Danube	D	Maipo	ND	Russian	ND	Volturno	D
Devoll	D	Malino	ND	Sabarmati	D	Wabash	ND
Dniester	D	Manimala	D	Saitama	ND	Wadiquena	ND
Don	ND	Mars1	ND	SaludaReevy	ND	WarregoValles2	D
Drin	ND	Mars2	ND	SanJoaquin	D	Wheeling	ND
EberswaldeDelta	D	Mars3	D	Sava	D	WolfBellCanyon	D
EberswaldeDelta2	D	Maule	ND	Schiapparelli	ND	Wyoming	ND
Ebro	ND	Meenachil	D	Seine	ND	Yangtze	D
EfestoFossae	D	Mekong	D	Simeto	ND	Yellowstone	ND
Elqui	ND	Meuse	D	Singkoyo	D	Yenisey	D
Eufrate	D	Mississippi	ND	Snake	ND	Zambezi	D
Gale	D	Missouri	D	StJoseph	D		
Ganges	ND	Moreau	D	Susquehanna	ND		
HuangHe	D	Muvattupuzha	D	Tambun	ND		

Table 1. Ground truth of drainage patterns. D= dendritic; ND= non-dendritic

In this section, I will show some of the results of our analysis using two DL models, VGGNet and AlexNet, for river drainage pattern classification. We systematically varied hyperparameters such as batch size, epochs, optimizers, kernel size, number of neurons and layers leading to diverse model performances. Tables accompany each model to outline the chosen hyperparameters and performance metrics, while ROC curves visually depict model discrimination capabilities. This approach provides a comprehensive view of how hyperparameters influence model performance in classifying river drainage patterns.

VggNET – exp 1	
Optimizer	Adam
Learning rate	0.0001
Kernel size	3x3
N. layers	7
Dense layer dimension	4096
N. neurons	4096
Batch size	20
Epochs	10

Table 2. VggNet model hyperparameters

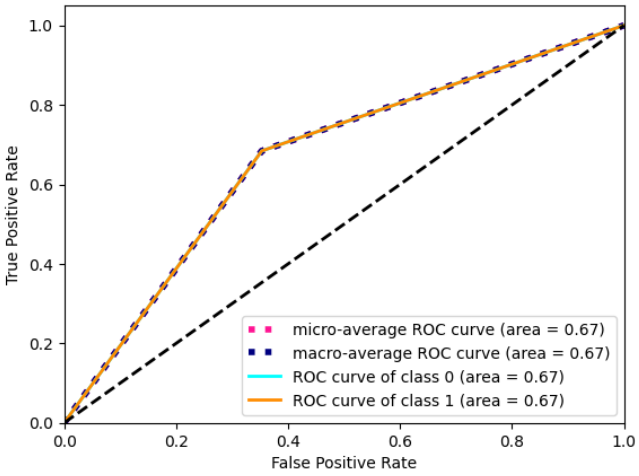

Fig 14. ROC curve related to exp. 1

	Precision	Recall	F1-score
Dendritic	65%	65%	65%
Mixed	68%	68%	68%

Table 2.1 Evaluation metrics of experiment 1

VggNET – exp 2	
Optimizer	Adam
Learning rate	0.0001
Kernel size	3x3
N. layers	7
Dense layer dimension	4096
N. neurons	4096
Batch size	1
Epochs	200

Table 3. VggNet model hyperparameters

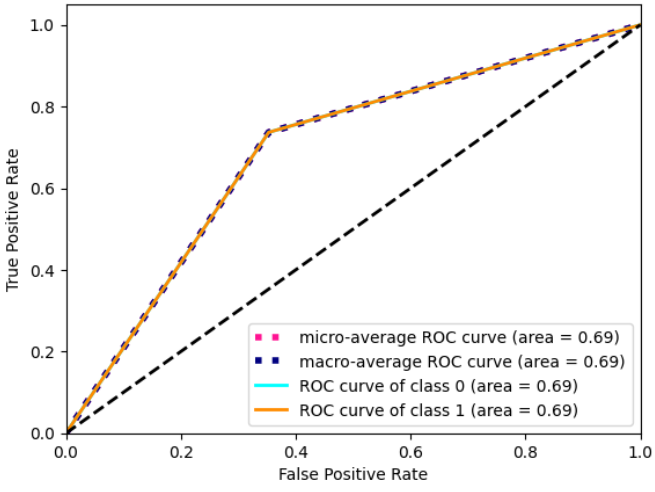

Fig 15. ROC curve related to the exp. 2

	Precision	Recall	F1-score
Dendritic	69%	65%	67%
Mixed	70%	74%	72%

Table 3.1 Evaluation metrics of experiment 2

VggNET – exp 3	
Optimizer	Adam
Learning rate	0.0001
Kernel size	3x3
N. layers	7
Dense layer dimension	4096
N. neurons	4096
Batch size	1
Epochs	20

Table 4. VggNet model hyperparameters

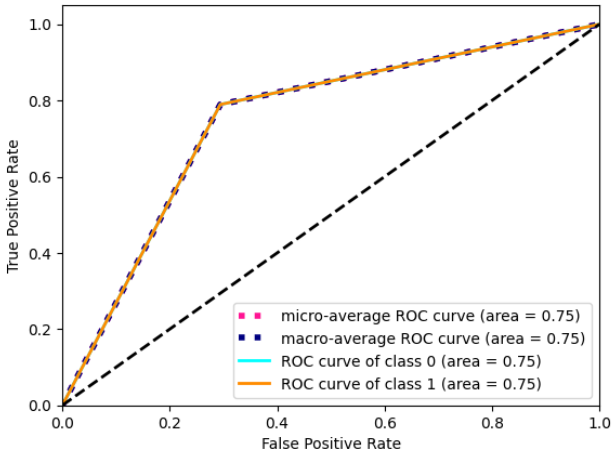

Fig 16. ROC curve related to exp.3

	Precision	Recall	F1-score
Dendritic	75%	71%	73%
Mixed	75%	79%	77%

Table 4.1 Evaluation metrics of experiment 3

VggNET – exp 4	
Optimizer	Adadelta
Learning rate	0.5
Kernel size	3x3
N. layers	7
Dense layer dimension	4096
N. neurons	4096
Batch size	1
Epochs	20

Table 5. VggNet model hyperparameters

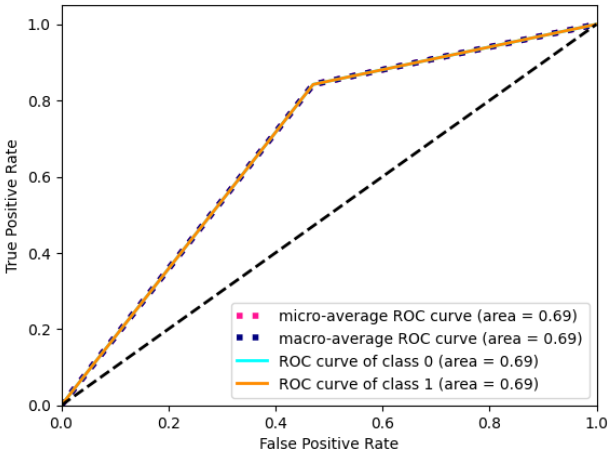

Fig 17. ROC curve related to exp.4

	Precision	Recall	F1-score
Dendritic	75%	53%	62%
Mixed	67%	84%	74%

Table 5.1 Evaluation metrics of experiment 4

In a series of experiments with the VGGNet model using the Adam optimizer, we systematically explored hyperparameters to optimize the classification of river drainage patterns, considering the challenges posed by a dataset containing noisy and complex images.

Parameter variations:

Learning rate (constant at 0.0001): We maintained a lower learning rate to ensure training stability, mitigating the risk of overshooting minima, especially with noisy data.

Neural Network Depth (minimum 7): To address noisy images, we increased the neural network's depth by adding more dense layers, enhancing its capacity to discern intricate patterns.

Batch size (varied between 1 and 20): To address noisy images, we increased the neural network's depth by expanding dense layers, enhancing its capacity to discern intricate patterns.

Epochs (varied between 1 and 200): Varying the number of training epochs allowed us to observe how the model behaved under different training durations.

Stride (kept constant at 1): Some parameters, like the stride, were kept constant during the experiments.

Performance metrics:

Precision reflects the accuracy of positive predictions (equation 2).

Recall measures the model's ability to capture all positive instances (equation 3).

F1-score provides a balanced assessment by harmonizing precision and recall (equation 4).

Experiment results:

1. **Experiment 1** yielded precision and recall values of around 65% to 68% for both Dendritic and Mixed patterns, indicating reasonably accurate positive predictions.

2. **Experiment 2** showed improved performance, with an increased F1-score (67% for Dendritic and 72% for Mixed), demonstrating a better balance between minimizing false positives and capturing true positives.

3. **Experiment 3** exhibited further improvements, achieving precision and recall values of up to 75% and F1-scores of 73% for both pattern types.

4. **Experiment 4** introduced the Adadelta optimizer, resulting in a significant recall increase (84%) for Mixed patterns but a decrease (41%) for Dendritic patterns, with an F1-score of 52% for Dendritic and 71% for Mixed.

ROC curve analysis:

Experiments with the Adam optimizer consistently achieved true positive rates (TPR) between 0.6 and 0.8, with corresponding false positive rates (FPR) around 0.3. This indicated the model's ability to accurately identify positive instances while maintaining a reasonably low rate of false positives.

Experiment 4 with the Adadelta optimizer produced a remarkable TPR exceeding 0.8 but with a slightly elevated FPR around 0.5, highlighting the optimizer's effectiveness in handling complex and noisy datasets.

In summary, these experiments provided valuable insights into parameter variations and their effects on model performance. Experiment 4, utilizing the Adadelta optimizer, showed promising results in accurately identifying Mixed patterns but with room for improvement in capturing Dendritic patterns. These findings contribute to the optimization of river drainage pattern classification in noisy images.

Moreover, we conducted a comparative analysis with a previous study that employed manual segmentation techniques. Interestingly, our approach, while yielding slightly lower TPR and higher FPR than the manual segmentation method, showcases competitive performance. This outcome is particularly noteworthy, as it suggests that our automated approach, despite its challenges, holds promise in handling noisy images and achieving commendable results.

It's essential to acknowledge that, in a comparative context, our experiments with automated segmentation yielded discrete results when contrasted with the previous work conducted by a scientific group using manual segmentation. In the latter, the absence of noise in the images allowed for more accurate results. However, it's crucial to note that our automated experiments hold promise, as they achieved commendable performance despite the inherent challenges of noisy images.

Our methodical exploration of hyperparameters, coupled with the introduction of the Adadelta optimizer with its higher learning rate, resulted in an experiment that outperformed the others, with a TPR exceeding 0.8. These findings underscore the intricate relationship between hyperparameters and optimizer selection and highlight the potential for optimized configurations to yield remarkable results in the classification of river drainage patterns, although they may not reach the same accuracy as manual segmentation in pristine conditions.

AlexNet – exp 5	
Optimizer	Adam
Learning rate	0.0004
Kernel size	3x3
N. layers	8
Dense layer dimension	4096
N. neurons	4096
Batch size	20
Epochs	80

Table 6. AlexNet model hyperparameters

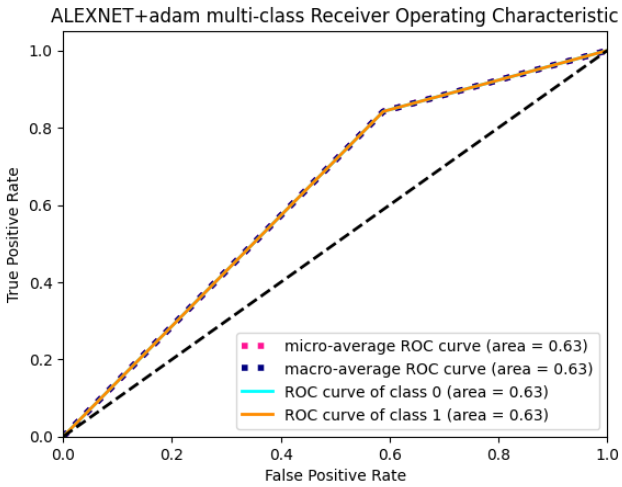

Fig 18. ROC curve related to exp. 5

	Precision	Recall	F1-score
Dendritic	70%	41%	52%
Mixed	62%	84%	71%

Table 6.1 Evaluation metrics of experiment 5

AlexNet – exp 6	
Optimizer	Adam
Learning rate	0.0004
Kernel size	3x3
N. layers	8
Dense layer dimension	4096
N. neurons	4096
Batch size	20
Epochs	40

Table 7. AlexNet model hyperparameters

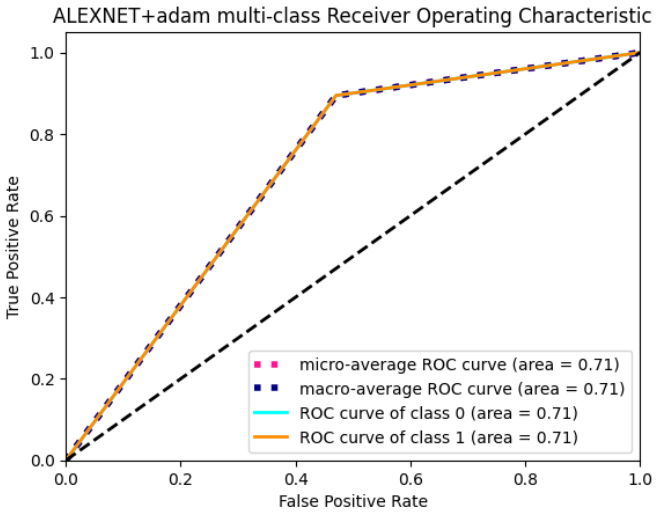

Fig 19. ROC curve related to exp. 6

	Precision	Recall	F1-score
Dendritic	82%	53%	64%
Mixed	68%	89%	77%

Table 7.1 Evaluation metrics of experiment 6

In the evaluation of AlexNet models with our automatic segmented images, noteworthy results were obtained, particularly considering the inherent noise present in the dataset.

In **experiment 1** (Figure 18) exhibited a false positive rate (FPR) of approximately 0.6 and a true positive rate (TPR) of approximately 0.85. The relatively elevated FPR could be attributed, in part, to the utilization of a high batch size. A larger batch size, while increasing computational efficiency, can introduce some level of granularity in the training process, potentially leading to suboptimal performance. Nonetheless, the results remained commendable, given the challenging dataset.

In **experiment 2** (Figure 19) showcased an even more remarkable performance, characterized by a TPR of approximately 0.9 and an FPR of approximately 0.4. This impressive result can be attributed to several factors. Firstly, the consistent use of the Adam optimizer effectively handled the dataset's complexities. Secondly, the architectural depth of AlexNet, exemplified by the network's eight layers, underscored the intrinsic power of AlexNet in learning hierarchical features and capturing intricate patterns.

Furthermore, it is crucial to highlight the substantial size of the dense layers within AlexNet. These layers, with a high number of artificial neurons, significantly contributed to the model's enhanced discriminative capacity compared to previous experiments conducted by a scientific group with manually segmented images. The amalgamation of architectural depth and substantial dense layers fortifies AlexNet's position as a formidable architecture for addressing complex computer vision tasks, especially when confronted with noisy datasets.

In summary, the AlexNet experiments demonstrated remarkable performance in classifying river drainage patterns in noisy images. Experiment 2 exhibited an impressive ability to correctly identify positive instances while maintaining a relatively low false positive rate, showcasing the power of AlexNet's architecture and substantial dense layers in handling complex computer vision tasks.

Finally, as a last significant comparison experiment, I ran the VggNET model with predetermined training and testing set. As for the training phase, only topographical images have been chosen, the ones present in the above-mentioned work prior to this one, in which those models were tested for the first time. It is noteworthy saying that in those past experiments, the models were trained on 131 manually segmented river images. This time I took the same 131 images, but automatic segmentation was applied to them, yielding discrete results in terms of quality, as already discussed in the “Image segmentation” subparagraph of this section. Of the 131 total images, 90% were reserved for training and only 10% have been used for validation. To really rest the model’s performance, a VggNET instance has then been tested against the 34 satellite images I collected, mainly from extraterrestrial bodies.

The results show similar performance to the previous experiments, indicating consistency between learning and testing patterns of VggNET. Given that AlexNET has a similar architecture to VggNET, we can assume

that the results would be similar. Unfortunately, due to technical reasons, I could not test this theory, although it is quite evident that this is somewhat always true.

VggNET – exp 7	
Optimizer	Adam
Learning rate	0.001
Kernel size	3x3
N. layers	7
Dense layer dimension	4096
N. neurons	4096
Batch size	20
Epochs	100

Table 8. VggNET model hyperparameters

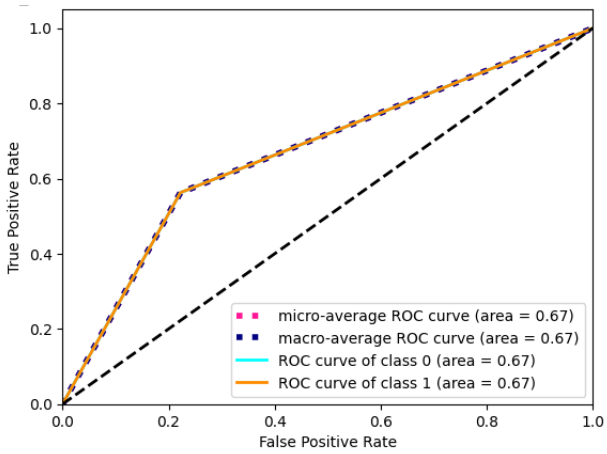

Fig 20. ROC curve related to exp. 7

	Precision	Recall	F1-score
Dendritic	67%	78%	72%
Mixed	69%	56%	62%

Table 8.1 Evaluation metrics of experiment 7

DISCUSSION

In this thesis, we embarked on a comprehensive exploration of image segmentation and classification techniques for terrestrial drainage networks and expanded our investigations to solar system bodies. Our primary goal was to develop robust methodologies capable of extracting and classifying river drainage patterns from diverse and noisy datasets.

The thesis began with an in-depth evaluation of segmentation methods, ultimately identifying a tailored approach that effectively removed artifacts from topographical images, setting the stage for subsequent analysis.

We then ventured into the domain of DL models, conducting systematic experiments with various hyperparameters and optimizers. The Adam optimizer emerged as a powerful choice, demonstrating impressive results with a high true positive rate (TPR) while maintaining a reasonable false positive rate (FPR). We explored two DL architectures, AlexNet and VGGNet, and found that AlexNet, with its eight layers and substantial dense layers, outperformed VGGNet, particularly excelling in handling complex computer vision tasks.

In comparison with previous manual segmentation work, our experiments yielded discrete results. However, our approach showed promise, especially considering the inherent challenges of noisy images. The synergy of architecture depth, dense layer size, and optimizer selection played pivotal roles in achieving commendable results.

This work represents a pioneering effort in the field, offering optimized segmentation methods and showcasing the potential of DL models in automated classification, even in noisy datasets. It opens new horizons for interdisciplinary exploration and objective classification in the study of geomorphological processes and beyond.

CONCLUSIONS

This pioneering work, while revealing some residual gaps, holds the promise of becoming a valuable tool to support the endeavors of geomorphologists, naturalists, and similar professionals. It offers a compelling alternative to traditional methodologies.
Despite initial challenges, the performance achieved through DL confirmed its capability to be applied to drainage patterns classification. It is important to note that, given the vast number of possible hyperparameter combinations, these results should be seen as a preliminary investigation, rather than a definitive outcome.

Further exploration of these parameter combinations, coupled with a more statistically consistent dataset, may hold the potential for even more significant advancements. Specifically, ongoing research is dedicated to enhancing automatic segmentation methods.
These improvements aim to refine the accuracy and efficiency of the segmentation process, ultimately yielding more precise representations of river drainage patterns, thus reducing the noise injected into the DL model training sets.

The objective recognition of river patterns enhances the study of geomorphological processes, which holds multidisciplinary importance. Taking the next step, standardizing classification through AI and expanding DL application, we plan to investigate a multi-class approach, tailoring classifications to specific drainage pattern types.

Moreover, we aim to initiate the search for an international nomenclature (a form of systematic naming) that uniquely identifies each morphology worldwide. This would facilitate a global focus on terrestrial processes and their relationships, particularly with Martian counterparts and those on other planets and satellites in our solar system.

REFERENCES

Al Sayem A., Chowdhury A. I., Shojol S. H., Mehedi M. H. K., Rasel A. A. 2023. “Implementing the Tesseract Method for Information Extraction from Images”, https://dl.acm.org/doi/abs/10.1145/3605423.3605431

Baker V.R., Hamilton C.W., Burr D.M., Gulick V.C., Komatsu G., Luo W., Rice Jr. J.W., Rodriguez J.A.P. 2015. “Fluvial geomorphology on Earth-like planetary surfaces: a review.” Geomorphology, 245: 149-182. https://www.ncbi.nlm.nih.gov/pmc/articles/PMC5701759/

Bishop C.M. 2006. “Pattern Recognition and Machine Learning. Information Science and Statistics.” New York Inc: Springer Nature. 319770394_Pattern_Recognition_and_Machine_Learning_Information_Science_and_Statistics

Breiman L. 2001. “Random Forest.” Machine Learning, 45: 5-32. https://link.springer.com/article/10.1023/A:1010933404324

Brescia M., Cavuoti S., Longo G. et al. 2014. “A Web Cyberinfrastructure for Astrophysical Data Mining.” The Astronomical Society of the Pacific, 126: 783-797. https://www.jstor.org/stable/10.1086/677725

Buffington J.M., Montgomery D.R. 2013. “Geomorphic Classification of Rivers.” Treatise on Geomorphology, 9: 730-767. https://www.fs.usda.gov/rm/pubs_other/rmrs_2013_buffington_j001.pdf

Buades A. 2005. “A non-local algorithm for image denoising.” IEEE Computer Society Conference on Computer Vision and Pattern Recognition, 60-65, https://ieeexplore.ieee.org/document/1467423

Canny J. 1986, “A Computational Approach to Edge Detection”, https://ieeexplore.ieee.org/document/4767851

Deng G., Broadbridge P. 2019. “Bregman inverse filter”, https://ietresearch.onlinelibrary.wiley.com/doi/full/10.1049/el.2018.7408

Donadio C. 2017. “Experimenting criteria for risk mitigation in fluvial-coastal environment.” Editorial, CSE Journal - City Safety Energy, 1: 9-14. https://journals.sagepub.com/doi/10.1177/030913319881108?icid=int.sj-full-text.similar-articles.3

Donadio, C., Brescia, M., Riccardo, A., Angora, G., Delli Veneri, M., & Riccio, G. (2021). “A novel approach to the classification of terrestrial drainage networks based on deep learning and preliminary results on solar system bodies.” Scientific Reports, 11, 5875. https://www.nature.com/articles/s41598-021-85254-x

Donadio C., Magdaleno F., Mazzarella A., Kondolf G.M. 2015. “Fractal dimension of the hydrographic pattern of three large rivers in the Mediterranean morphoclimatic system: geomorphologic interpretation of Russian (USA), Ebro (Spain) and Volturno (Italy) fluvial geometry.” Pure and Applied Geophysics, 172: 1975-1984. https://link.springer.com/article/10.1007/s00024-014-0910-z

Goodfellow I., Bengio Y., Courville A. 2016. “Deep Learning.” Switzerland: Springer-Nature. http://alvarestech.com/temp/deep/Deep%20Learning%20by%20Ian%20Goodfellow,%20Yoshua%20Bengio,%20Aaron%20Courville%20(z-lib.org).pdf

Hanley J.A., McNeil B.J. 1982. “The Meaning and Use of the Area Under a Receiver Operating Characteristic (ROC) Curve.” Radiology, 143: 29-36. https://pubmed.ncbi.nlm.nih.gov/7063747/

Howard A.D. 1967. “Drainage Analysis in Geologic Interpretation: A Summation.” American Association of Petroleum Geologist Bulletin, 51: 2246-2259. https://www.scirp.org/(S(czeh2tfqyw2orz553k1w0r45))/reference/ReferencesPapers.aspx?ReferenceID=1130746

Horton R.E. 1945. “Erosional development of streams and their drainage basins: hydrophysical approach to quantitative morphology.” Bulletin of the Geological Society of America, 56: 275-270. https://www.scirp.org/(S(czeh2tfqyw2orz553k1w0r45))/reference/ReferencesPapers.aspx?ReferenceID=1451620

Kondolf G.M., Piégay H. 2016. “Tools in Fluvial Geomorphology.” New Jersey: Wiley-Blackwell. Lary D.J. 2010. Artificial Intelligence in Aerospace. https://www.researchgate.net/publication/283625816_Tools_in_Fluvial_Geomorphology_Problem_Statement_and_Recent_Practice

Krizhevsky A., Sutskever I., Hinton G. E. 2012. “Imagenet classification with deep convolutional neural networks”, https://scholar.google.com/citations?view_op=view_citation&hl=en&user=xegzhJcAAAAJ&citation_for_view=xegzhJcAAAAJ:u5HHmVD_uO8C

LeCun Y., Boser B., Denker J.S. et al. 1989. “Backpropagation applied to handwritten zip code recognition.” Neural Computation, 1: 541-551. https://ieeexplore.ieee.org/document/6795724

Palucis M.C., Dietrich W.E., Williams R.M.E., Hayes A.G., Parker T., Sumner D.Y., Mangold N., Lewis K., Newsom H. 2016. “Sequence and relative timing of large lakes in Gale crater (Mars) after the formation of Mount Sharp.” Journal of Geophysical Research: Planets, 121: 472-496. https://agupubs.onlinelibrary.wiley.com/doi/10.1002/2015JE004905

Paik K., Kumar P. 2010. “Optimality approaches to describe characteristic fluvial patterns on landscapes.” Philosophical transactions of the Royal Society of London. Series B, Biological sciences, 365: 1387-95. https://www.ncbi.nlm.nih.gov/pmc/articles/PMC2871905/

Pereira-Claren A., Gironás J., Niemann J.D., Passalacqua P., Mejia A., Escauriaza C. 2019. “Planform geometry and relief characterization of drainage networks in high-relief environments: An analysis of Chilean Andean basins.” Geomorphology, 341: 46-64. https://repositorio.uc.cl/server/api/core/bitstreams/d5313040-a196-4894-8bab-7ead8898569b/content

Perona P., Malik J. 1987. “Scale-space and edge detection using anisotropic diffusion.” Proceedings of IEEE Computer Society Workshop on Computer Vision, 16-22

Shen D., Wu G., Il Suk H. 2017. “Deep Learning in Medical Image Analysis.” Annual Review of Biomedical Engineering, 19: 221-248. https://www.annualreviews.org/doi/10.1146/annurev-bioeng-071516-044442

Simonyan K., Zisserman A. 2014. “Very Deep Convolutional Networks for Large-Scale Image Recognition”, https://arxiv.org/abs/1409.1556

Starck J.L., Murtagh F. 2006. “Handbook of Astronomical Data Analysis.” New York Inc: Springer-Nature. https://www.academia.edu/2608657/Handbook_of_Astronomical_Data_Analysis

Sowparnika M., Jairaj P.G. 2014. “Implication of fractal dimension of properties of rivers and rivers basin.” International Journal of Civil Engineering and Technology (IJCIET), 5: 155-164. https://sdbindex.com/Documents/index/00000001/00000-49957

Stehman S.V. 1997. “Selecting and interpreting measures of thematic classification accuracy.” Remote Sensing of Environment, 62: 77-89. https://www.sciencedirect.com/science/article/abs/pii/S0034425797000837

Stepinski T.F., Marinova M.M., McGovern P.J., Clifford S.M. 2002. “Fractal analysis of drainage basins on Mars.” Geophys. Res, 29, 1189. https://agupubs.onlinelibrary.wiley.com/doi/pdf/10.1029/2002GL014666

Turcotte D.L. 1997. “Fractals and Chaos in Geology and Geophysics.” Cambridge: Cambridge University Press. https://www.cambridge.org/core/books/fractals-and-chaos-in-geology-and-geophysics/FA8339855DBBF054CCF18D8E5DDFFAC9

Vijayan D. 2014. “Basin asymmetry and associated tectonics: A case study of Achankovil river basin, Kerala.” Transactions of the Institute of Indian Geographers, 36: 207-215.

https://www.researchgate.net/publication/287343428_Basin_asymmetry_and_associated_tectonics_A_case_study_of_Achankovil_river_basin_Kerala

Wilcock P.R., Iverson R.M. 2003. “Prediction in geomorphology.” Washington: American Geophysical Union. https://pubs.usgs.gov/publication/70226935

Wood L.J. 2006. “Quantitative geomorphology of the Mars Eberswalde delta.” GSA Bulletin, 118:557-566. https://www.researchgate.net/publication/249527402_Quantitative_geomorphology_of_the_Mars_Eberswalde_delta

Gosk Z.E., Wołk K., Czarnowski W. 2019. “Deep Learning in State-of-the-Art Image Classification Exceeding 99% Accuracy.” In: New Knowledge in Information Systems and Technologies, Rocha A., Adeli H., Reis L.P., Costanzo S. (Editors). Pp.946-957. https://www.researchgate.net/publication/332027696_Deep_Learning_in_State-of-the-Art_Image_Classification_Exceeding_99_Accuracy